

A Molecular Orbital Rationalization of Ligand Effects in N₂ Activation

Alireza Ariafard,^{*[a]} Nigel J Brookes,^[a] Robert Stranger,^[b] and Brian F Yates^{*[a]}

Abstract: Molecular orbital theory has been used to study a series of $[(\mu\text{-N}_2)\text{-ML}_3]_2$ complexes as models for dinitrogen activation, with $M = \text{Mo, Ta, W, Re}$ and $L = \text{NH}_2, \text{PH}_2, \text{AsH}_2, \text{SbH}_2$ and $\text{N}(\text{BH}_2)_2$. The main aims of this study have been to provide a thorough electronic analysis of the complexes and to extend previous work involving molecular orbital analyses. Molecular orbital

diagrams have been used to rationalize why for $L = \text{NH}_2$ ligand rotation is important for the singlet state but not the triplet, to confirm the effect of ligand π

Keywords: density functional calculations • ligand rotation • molecular orbital theory • nitrogen activation • reaction mechanisms

donation, and to rationalize the importance of the metal d-electron configuration. The outcomes of this study will assist with a more in-depth understanding of the electronic basis for N₂ activation and allow clearer predictions to be made about the structure and multiplicity of systems involved in transition-metal catalysis.

Introduction

The activation of the nitrogen molecule in the laboratory remains an important and popular problem in science due to the intellectual challenge and the significant industrial benefits that would flow from a mild low-cost process.^[1,2] One promising avenue is the use of three-coordinate molybdenum complexes, and the mechanism of the Mo^{III}-promoted N₂ bond cleavage reaction has been extensively studied by experimentalists^[3–5] and theoreticians^[6–8] during the past decade. As shown in Figure 1, the proposed mechanism of the reaction includes the initiation step via the end-on coordination of N₂ to a quartet molybdenum reactant followed by an intersystem crossing process from the quartet to the doublet surface. The system then involves the coupling of the doublet encounter Mo complex with a second molybdenum reactant, giving rise to the triplet dinuclear intermediate $[(\mu\text{-N}_2)(\text{MoL}_3)_2]$. Finally, the N₂ bond cleaves via the singlet transition state shown in Figure 1 preceded by a spin

flip from the triplet to the singlet state. The calculations showed that the stability of the singlet $(\mu\text{-N}_2)(\text{MoL}_3)_2$ relative to the triplet analogue mainly depends on the nature of the ancillary ligands L. In general, the stronger the π -donating capability of L, the smaller the triplet–singlet energy gap of $[(\mu\text{-N}_2)(\text{MoL}_3)_2]$, and consequently, the smaller the rate-determining barrier.^[6,8,9]

The theoretical studies on the $[(\mu\text{-N}_2)\{\text{Mo}(\text{NH}_2)_3\}_2]$ intermediate were also applied to investigate the dependence of the energy of the intermediate on the NH₂ ligand orientation around the Mo metal centers. Two different structures with D_{3d} and C_{2h} symmetries were found for the triplet intermediate. The D_{3d} form having trigonal symmetry around each metal was calculated to be approximately 4 kJ mol⁻¹ higher in energy than the C_{2h} form having one NH₂ ligand at each Mo metal center rotated by 90°. In comparison, the energy difference between the D_{3d} and C_{2h} forms is much more pronounced for the singlet intermediate $[(\mu\text{-N}_2)\{\text{Mo}(\text{NH}_2)_3\}_2]$. The singlet C_{2h} form was found to be 56 kJ mol⁻¹ more stable than the singlet D_{3d} form. The calculations at the BP86 level revealed that the ligand rotation brings the singlet C_{2h} form 13 kJ mol⁻¹ below the triplet D_{3d} form.^[10]

In addition, the replacement of one of the d³ Mo metal centers with the d² Nb metal center yielded some interesting results. Contrary to the very small singlet–triplet energy gap reported for the Mo^{III}Mo^{III} intermediate, the corresponding doublet–quartet energy gap for the Mo^{III}Nb^{III} intermediate was calculated to be substantially large. Christian and Stanger calculated a value of 132 kJ mol⁻¹ in favor of the doublet.^[11] The NH₂ ligand rotation also plays a crucial role in

[a] Dr. A. Ariafard, N. J. Brookes, Prof. B. F. Yates
School of Chemistry, University of Tasmania
Private Bag 75, Hobart TAS 7001 (Australia)
Fax: (+61)3-6226-2858
E-mail: ariafard@yahoo.com
Brian.Yates@utas.edu.au

[b] Prof. R. Stranger
Department of Chemistry, Australian National University
Canberra ACT 0200 (Australia)

Supporting information for this article is available on the WWW under <http://www.chemeurj.org/> or from the author.

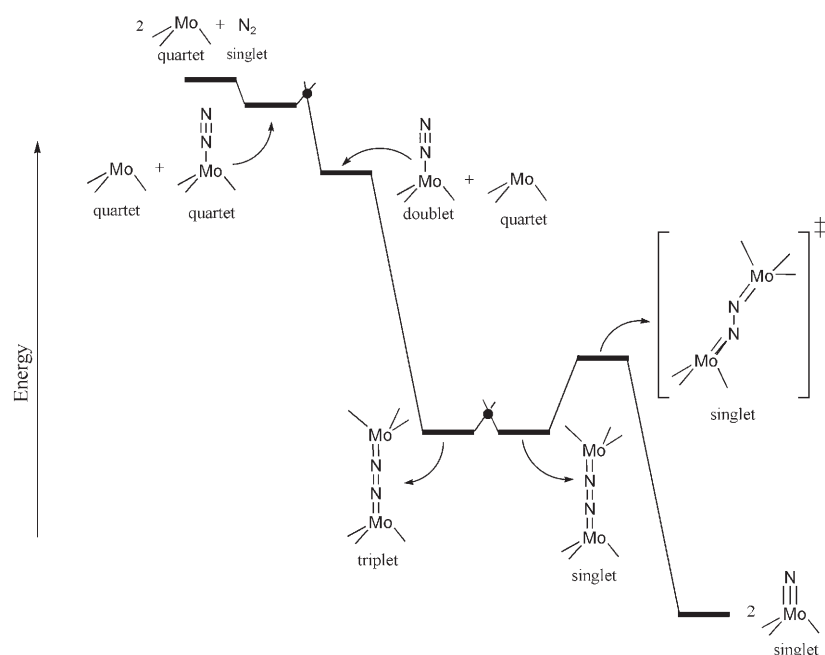


Figure 1. Potential energy surface for reaction of N_2 with $2 MoL_3$.

stabilizing the doublet $Mo^{III}Nb^{III}$ intermediate. The calculations showed that the doublet intermediate bearing the rotated NH_2 ligands is 47 kJ mol^{-1} more stable than the corresponding non-rotated intermediate.^[10]

The main purpose of the present study is to theoretically rationalize why the NH_2 rotation is an important process for the stabilization of the singlet $Mo^{III}Mo^{III}$ intermediate and not the triplet analogue. The dependence of the triplet–singlet energy gap on the d-electron configuration of the metal center has been examined by performing additional calculations on the model intermediates $[(\mu-N_2)\{M(NH_2)_3\}_2]$ for $M=Ta, W,$ and Re . The effect of the ancillary ligand L on the triplet–singlet energy gap of $[(\mu-N_2)(ML_3)_2]$ has also been investigated. Overall this paper addresses the dependence of the structure and multiplicity on the transition metal and its ligands and allows rational predictions to be made.

Results and Discussion

π -Donor ability of L : Calculations^[12] were carried out starting with the triplet and singlet states of $[(\mu-N_2)(MoL_3)_2]$, where $L=NH_2, PH_2, AsH_2, SbH_2,$ and $N(BH_2)_2$.^[13] The π -donor ability of L decreases from N to Sb . In each case, we have used non-rotated species as the starting points of the geometry optimizations. N_X is the nomenclature used for the studied species where $X=S$ stands for singlet, $X=D$ for doublet, $X=T$ for triplet, and $X=Q$ for quartet spin states. The results given in Figure 2 show that the singlet form for $L=NH_2$ and PH_2 is more stable than the corresponding triplet, whereas for $L=AsH_2, SbH_2,$ and $N(BH_2)_2$ the triplet form is more stable. It follows from this result that, as expected, the triplet–singlet energy gap is mainly reliant on

the π -donating capability of L . Apparently the strong π -donor ligands enhance the stability of the singlet form relative to the triplet form. A comparison of the frontier molecular orbitals^[4,6,14,15] for the singlet and triplet forms provides insight into the origin of this issue. Figure 3 shows an MO diagram for interactions between valence orbitals of N_2 and in- and out-of-phase combinations of d-valence orbitals of two $Mo(NH_2)_3$ units. Note that the lowest energy valence orbital of N_2 is not shown. In addition, π_1 and π_2 have a weak stabilizing interaction with the metal d orbitals, but they remain essentially as π orbitals on N_2 and are omitted from the central part of the diagram

L	Species	$\Delta E_{S,T}$ [kJ mol ⁻¹]
NH_2	1	-11.7
PH_2	2	-1.7
AsH_2	3	50.6
SbH_2	4	52.7
$N(BH_2)_2$	5	59.8

Figure 2. Singlet–triplet energies for a variety of ligands L .

for clarity. The occupied **MO1** and **MO2** orbitals are primarily derived from interaction of the out-of-phase combination of d_{z^2} orbitals with σ_2 on N_2 , and of in-phase combinations of d_{z^2} orbitals with σ_3 on N_2 , respectively. The $d_{xz}-d_{xz}$ and $d_{yz}-d_{yz}$ orbitals combine with the unoccupied π_1^* and π_2^* orbitals, respectively, forming the degenerate **MO3** and **MO4** orbitals. The in-phase combinations of d_{xz} ($d_{xz} + d_{xz}$) and d_{yz} ($d_{yz} + d_{yz}$) orbitals are slightly destabilized due to the repulsive interaction with the low-lying occupied π_1 and π_2 orbitals on N_2 . In the triplet dinuclear intermediate $[(\mu-N_2)(MoL_3)_2]$, the **MO5** and **MO6** orbitals are degenerate and singly occupied (Figure 3). This indicates that, without taking into account the ancillary ligand L , the triplet form should be electronically far more favorable than the singlet. Therefore, we can say that the singlet species **3_S**, **4_S**, and **5_S** are higher in energy than their triplet counterparts as a result of the violation of Hund's rule.

Rotation of L —singlet case: The most important question now is why the dinuclear intermediates $[(\mu-N_2)(MoL_3)_2]$

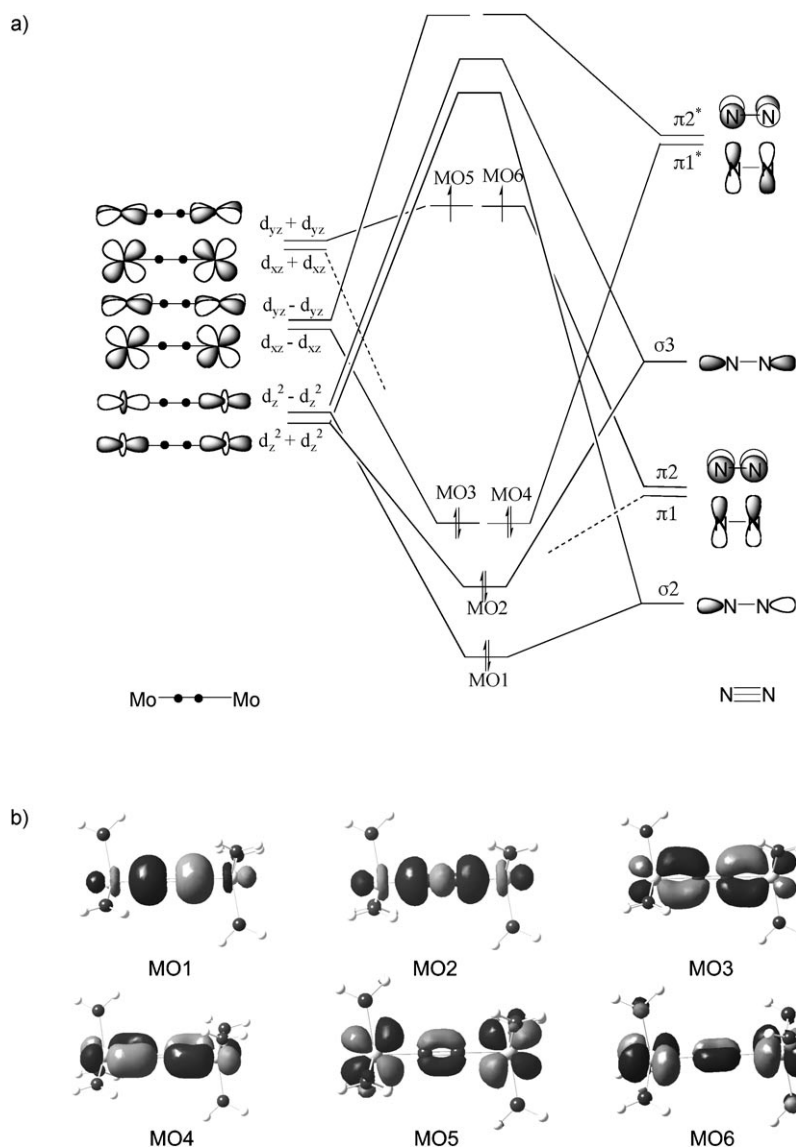


Figure 3. a) Schematic orbital correlation diagram showing the σ and π interactions between the valence orbitals of 2MoL_3 and N_2 for $[(\mu\text{-N}_2)\{\text{ML}_3\}_2]$. b) Spatial plots of the molecular orbitals MO1–MO6 for the model complex $[(\mu\text{-N}_2)\{\text{M}(\text{NH}_2)_3\}_2]$.

with the strong π -donor ligands can violate Hund's rule and yet be more stable than their triplet counterpart. An analysis of the interaction between the Mo metal centers and the L ligands provides an excellent probe for understanding of this issue. As mentioned above, the NH_2 ligand rotation at each Mo metal center by 90° plays a crucial role in stabilizing the singlet intermediate $[(\mu\text{-N}_2)\{\text{Mo}(\text{NH}_2)_3\}]$. Indeed, the ligand rotation provides the best orientation for the nitrogen lone pair electrons to interact with the Mo d_{xz} orbitals. The in-phase combination of the lone pair orbitals (**n1**) pushes up **MO3** in energy (Figure 4), enhancing metal-to- N_2 charge transfer and leading to an increase in N_2 activation. This pull–push interaction builds up the electron density in the N_2 p_x orbitals more than in the N_2 p_y orbitals, yielding a zigzag arrangement for the singlet state of $[(\mu\text{-N}_2)\{\text{Mo}$

$(\text{NH}_2)_3\}]$ (**1_S** in Figure 5). A NBO analysis shows that the N_2 p_x orbital populations (2.434 e) is 0.102 larger than the N_2 p_y orbital populations (2.332 e). The out-of-phase combination of the lone pair orbitals (**n2**) in the singlet intermediate is stabilized by interaction with the unoccupied **MO5** orbital (Figure 4). This interaction is accompanied by a slight shortening of the Mo–N3 and Mo–N6 bond lengths, due to an increase in the strengths of the Mo–N3 and Mo–N6 bonds (Figure 5). It can also be clearly seen from Figure 5 that the rotation also leads to a shortening of the Mo–N1, Mo–N2, Mo–N4, and Mo–N5 bonds, indicating a stabilization of all the Mo–N bonds. The orbital interaction diagram shown in Figure 6 explains why the rotation strengthens the four Mo–N bonds. In the non-rotated intermediate, there is a competition between the lone pair electrons of the three nitrogen atoms at each Mo metal center to interact with the empty $d_{x^2-y^2}$ and d_{xy} orbitals of Mo. This feature leads to a dilution of the Mo–N bonding interactions. The relevant rotation turns off the competition and facilitates charge transfer from the remaining two nitrogen atoms to Mo, making the Mo–N bonds stronger. Therefore

the stronger Mo–N bonds in **1_S** can compensate for the destabilization effect of the Columbic repulsion between the two electrons in orbital **MO6**, giving rise to higher stability of **1_S** relative to **1_T**.

To support the argument that the rotated NH_2 ligand enhances the charge transfer from the lone pair electrons of NH_2 moieties to the Mo metal centers, we performed partial geometry optimizations on the singlet intermediate by fixing the dihedral angles listed in Table 1. The results of the calculations show that the NH_2 rotation from $\theta=90$ to 10° brings about a significant destabilization (43.9 kJ mol^{-1}). The attempts to locate a structure with $\theta=0^\circ$ were unsuccessful. The lone pair orbital population of NH_2 (obtained from NBO analysis) gradually increases as the dihedral angle θ decreases. There exists a very good correlation between the

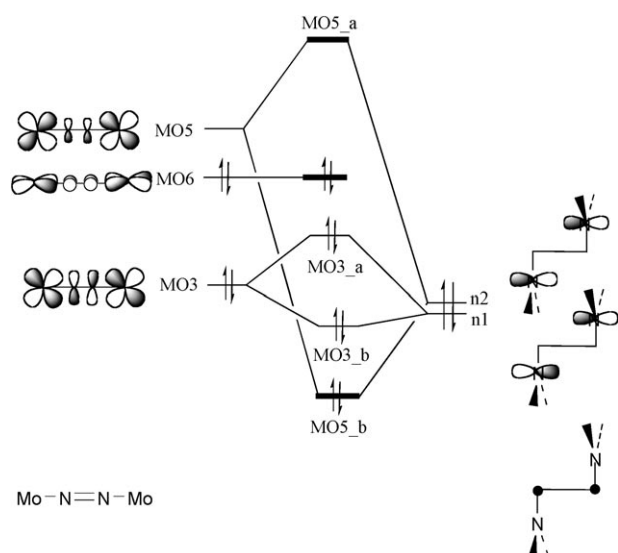


Figure 4. Schematic orbital correlation diagram showing the π interactions between the valence orbitals of the MoN_2Mo fragment and the in-phase and out-of-phase combinations of the rotated NH_2 fragments.

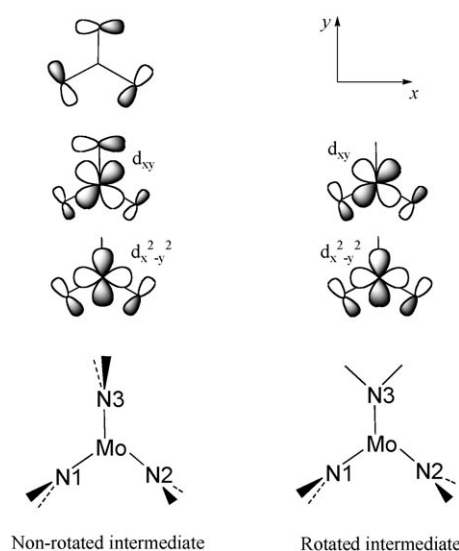


Figure 6. Interaction of ligand and metal orbitals in rotated and non-rotated intermediates.

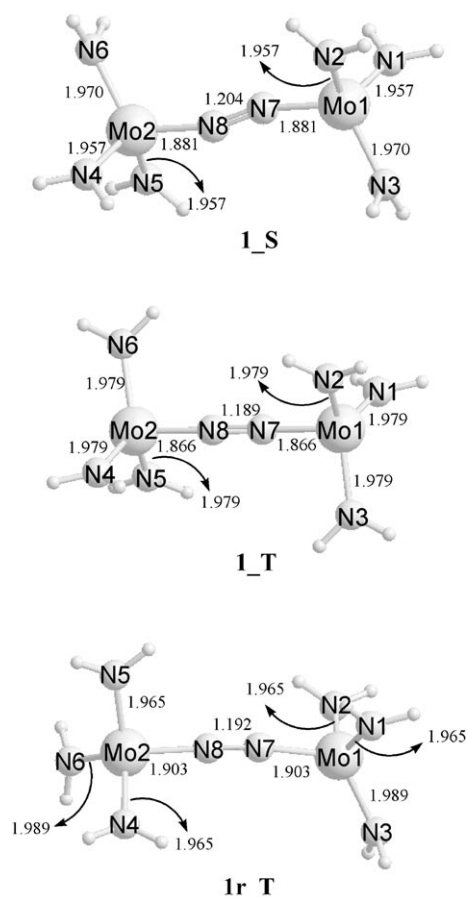


Figure 5. Selected structural parameters [\AA] calculated for the species **1_S**, **1_T**, **1_{r_T}**.

relative energy of partially optimized structures and the averaged population of the lone pair orbital of the NH_2 moi-

eties. The largest HOMO–LUMO gap is calculated for the structure with $\theta=90^\circ$, whereas the smallest is calculated for the structure with $\theta=10^\circ$. On the basis of the molecular orbital diagram given in Figure 4, one can expect that the NH_2 rotation is able to further destabilize the LUMO, giving the larger HOMO–LUMO gap. The larger the HOMO–LUMO gap, the greater the stability of the singlet intermediate relative to the triplet. The stronger push–pull π -interactions in the structures with larger dihedral angle θ (Figure 4) are also capable of enhancing the metal-to- N_2 charge transfer as evidenced by the smaller N_2 partial charges as well as the longer N–N distances (Table 1).

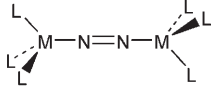
Rotation of L–triplet case: Consistent with the previously detailed theoretical studies,^[16] the rotation of a NH_2 ligand at each metal center of **1_T** results in a structure (**1_{r_T}**, Figure 5) lying 13.8 kJ mol^{-1} below **1_T**. This result reflects the much lower sensitivity of the triplet non-rotated intermediate to the ligand rotation as compared to its singlet analogue. The Mo1–N1, Mo1–N2, Mo2–N4, and Mo2–N5 bond lengths in **1_{r_T}** are 0.014 \AA shorter than those in **1_T**, whereas the Mo1–N3, and Mo2–N6 bond lengths in **1_{r_T}** are 0.010 \AA longer (Figure 5) (although these changes in bond length are probably within the error margin of the calculations). The averaged population of the lone pair orbitals of N1, N2, N4, and N5 in **1_{r_T}** (1.578) is 0.043 less than that in **1_T** (1.621), whereas the average for N3 and N6 in **1_{r_T}** (1.653) is 0.031 more. These results imply that the ligand rotation causes an increase in the charge transfer from N1, N2, N4, and N5 to Mo, whereas it causes a decrease in the charge transfer from N3 and N6 to Mo. Therefore, the Mo1–N1, Mo1–N2, Mo2–N4, and Mo2–N5 bonds in **1_{r_T}** become stronger than those in **1_T**, whereas the Mo1–N3, and Mo2–N6 bonds in **1_{r_T}** become weaker. From this comparison, one may conclude that the strengthening of the Mo1–N1, Mo1–N2, Mo2–N4, and Mo2–N5 bonds in **1_{r_T}** is

Table 1. Relative energy, HOMO–LUMO gap, the averaged population of the lone pair orbitals of N3 and N6 (Pop 1), the averaged population of the lone pair orbitals of N1, N2, N4, and N5 (Pop 2), N₂ NBO charge, and N–N bond length with a variety of dihedral angles θ .

θ [°]	Relative energy [kJ mol ⁻¹]	HOMO–LUMO gap [eV]	Pop 1	Pop 2	N ₂ NBO charge	N–N bond length [Å]
90	0.0	1.776	1.585	1.579	+0.326	1.198
80	1.6	1.774	1.588	1.580	+0.332	1.198
70	6.2	1.771	1.591	1.582	+0.346	1.197
60	12.9	1.769	1.596	1.585	+0.370	1.196
50	20.3	1.729	1.602	1.590	+0.408	1.194
40	26.9	1.654	1.607	1.595	+0.448	1.193
30	32.3	1.570	1.609	1.600	+0.475	1.192
20	37.6	1.455	1.611	1.604	+0.500	1.192
10	43.9	1.330	1.616	1.607	+0.562	1.192

able to counterbalance the weakening of the Mo1–N3, and Mo2–N6 bonds, giving rise to a comparable stability for **1_T** and **1r_T**. A crucial reason for the weakening of the Mo1–N3, and Mo2–N6 bonds in **1r_T** can be attributed to the single occupation of orbital **MO5_a** having a Mo–N π -antibonding character (Figure 4).

Metal electronic configuration (d⁴ vs. d³ vs. d² vs. d¹): We also considered model systems $[(\mu\text{-N}_2)\{\text{ML}_3\}_2]$ with M = Ta, W, and Re (L = NH₂, AsH₂) to elucidate the effect of metal electron configuration on the triplet–singlet energy gap (Figure 7). As with the Mo systems, the stability of the singlet form of $[(\mu\text{-N}_2)\{\text{WL}_3\}_2]$ relative to its triplet is primarily ligand-dependent. For example, the **8_S** structure is 31.1 kJ mol⁻¹ more stable than **8_T**, while **9_S** is 24.0 kJ mol⁻¹ less stable than **9_T**. Interestingly, for the d²d² Ta^{III}Ta^{III} and d⁴d⁴ Re^{III}Re^{III} systems, irrespective of whether the L ligand is a strong or weak π -donor, the singlet structure is lower in energy than the corresponding triplet analogue. The MO diagram given in Figure 3 explains the large



M	L	Species	ΔE_{S-T} [kJ mol ⁻¹]
M = Ta	NH ₂	6	-195.1
	AsH ₂	7	-158.7
M = W	NH ₂	8	-31.1
	AsH ₂	9	24.0
M = Re	NH ₂	10	-40.9
	AsH ₂	11	-28.2

Figure 7. Singlet–triplet energies for a series of transition metals.

drop of the singlet energy in the Ta^{III}Ta^{III} and Re^{III}Re^{III} systems. For the singlet Ta^{III}Ta^{III} systems, the **MO3** and **MO4** π -bonding orbitals correspond to the HOMO. In the case of the triplet, one of these electrons is forced into one of the high lying unoccupied orbitals with an antibonding character, resulting in the much higher instability of **6_T** (195.1 kJ mol⁻¹) and **7_T** (158.7 kJ mol⁻¹). For the singlet Re^{III}Re^{III} systems, the doubly occupied **MO5** and **MO6** orbitals correspond to the HOMO. The lower stability of the triplet Re^{III}Re^{III} systems relative to their singlet counterparts is likely due to moving one electron from a weakly antibonding orbital to a significantly antibonding orbital, but as expected this has a lesser effect on the relative energy than moving an electron from a bonding to antibonding orbital as in the Ta^{III}Ta^{III} case.

Since both the **MO5** and **MO6** orbitals are unfilled in the singlet form of $[(\mu\text{-N}_2)\{\text{Ta}(\text{NH}_2)_3\}_2]$, it was found that only the rotated form (**6_S**) corresponds to a minimum on the potential energy surface (PES) (Figure 8). On the contrary, the results of our calculations show that the singlet non-rotated form of $[(\mu\text{-N}_2)\{\text{Re}(\text{NH}_2)_3\}_2]$ (**10n_S**) forms a stable minimum on the PES. This conformer lies only 7.8 kJ mol⁻¹ above the rotated singlet form of $[(\mu\text{-N}_2)\{\text{Re}(\text{NH}_2)_3\}_2]$ (**10_S**). The formation of **10_S** is relatively disfavored by the repulsive interaction derived from the double occupancy of **MO5_a** (Figure 4). The effect of the repulsive interaction in **10_S** is clearly evidenced by the calculated N3–Mo1–N7 and N6–Mo2–N8 bond angles, which are significantly larger by 18.1–43.7° than in **10n_S** and **6_S** (Figure 8). In other words, the N3–Mo1–N7 and N6–Mo2–N8 angles in **10_S** are widened to avoid the four-electron repulsion.

For completeness, we also calculated the triplet–singlet energy gap in a d¹d¹ model system with N₂ bridging end-on between two HfL₃ (L = AsH₂ and NH₂). Our calculations on $[(\mu\text{-N}_2)\{\text{HfL}_3\}_2]$ predict a triplet ground state for these systems, with triplet–singlet energy gaps of 44.2 kJ mol⁻¹ for L = NH₂ and 40.5 for L = AsH₂. In $[(\mu\text{-N}_2)\{\text{HfL}_3\}_2]$, the highest occupied molecular orbitals **MO3** and **MO4** are degenerate and singly occupied. This degeneracy means that there is a strong preference for the triplet form to be the ground state for $[(\mu\text{-N}_2)\{\text{HfL}_3\}_2]$.

Some comments about the d³d² Mo^{III}Nb^{III} system: As mentioned in the Introduction, the doublet form of $(\text{NH}_2)_3\text{MoN}_2\text{Nb}(\text{NH}_2)_3$ is 132 kJ mol⁻¹ more stable than its quartet counterpart.^[11] The lower stability of the quartet state in the d³d² Mo^{III}Nb^{III} system is conveniently related to

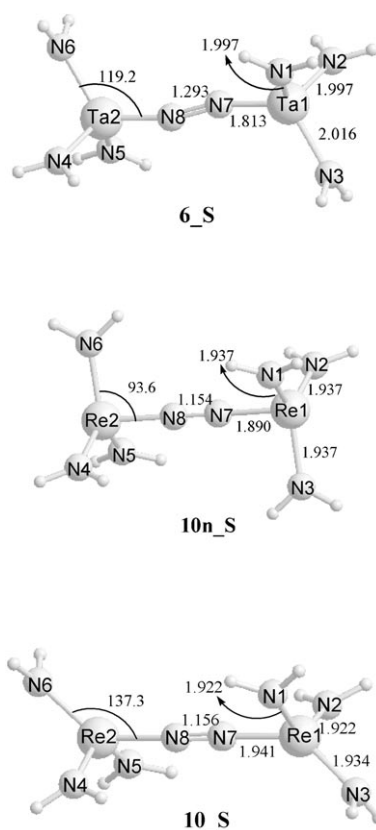


Figure 8. Selected structural parameters [Å, °] calculated for the species **6_S**, **10n_S**, **10_S**.

the depopulation of the π -bonding orbitals shown in Figure 5. The previous experimental^[17] and theoretical^[10] studies showed that the rotation of one amide ligand at the Nb moiety is much more important than at the Mo moiety. This behavior is understandable if one inspects the frontier orbitals of $[(\text{NH}_2)_3\text{MoN}_2\text{Nb}(\text{NH}_2)_3]$. It should be noted that the orbitals shown in Figure 3 for the case of $[(\text{NH}_2)_3\text{MoN}_2\text{Nb}(\text{NH}_2)_3]$ are somewhat different from $[(\text{NH}_2)_3\text{MoN}_2\text{Mo}(\text{NH}_2)_3]$. The **MO5** and **MO6** orbitals in the $\text{Mo}^{\text{III}}\text{Nb}^{\text{III}}$ system are unsymmetrical in that the d orbitals of Nb contribute more to these molecular orbitals than the d orbitals of Mo. On the basis of Mulliken population analyses,^[18] the percentage contributions of Nb and Mo in **MO5** are calculated as 41% and 36%, respectively, and in **MO6** 42% and 35%, respectively. A reverse order is found for **MO3** and **MO4**; 17% for Nb versus 40% for Mo in **MO3** and 12% for Nb versus 31% for Mo in **MO4**. This can be

explained in terms of the different energy levels of the frontier orbitals in $\text{Nb}(\text{NH}_2)_3$ and $\text{Mo}(\text{NH}_2)_3$. Because the d orbitals of $\text{Nb}(\text{NH}_2)_3$ are higher in energy than those of $\text{Mo}(\text{NH}_2)_3$, the Nb d_{xz} and d_{yz} orbitals contribute much more to **MO5** and **MO6** but much less to **MO3** and **MO4**. A greater contribution of Nb to **MO5** leads to a better interaction between the rotated amide ligand and Nb, making the rotation more pronounced at the Nb moiety.

Acknowledgements

We would like to thank the Australian Research Council (ARC) for project funding. We are also indebted to the Australian Partnership for Advanced Computing (APAC) and the Tasmanian Partnership in Advanced Computing (TPAC) for a generous time grant on their parallel computing facilities.

- [1] R. R. Schrock, *Chem. Commun.* **2003**, 2389–2391.
- [2] B. MacKay, M. Fryzuk, *Chem. Rev.* **2004**, *104*, 385–401.
- [3] C. E. Laplaza, C. C. Cummins, *Science* **1995**, *268*, 861–863.
- [4] C. E. Laplaza, M. J. A. Johnson, J. C. Peters, A. L. Odom, E. Kim, C. C. Cummins, G. N. George, I. J. Pickering, *J. Am. Chem. Soc.* **1996**, *118*, 8623–8638.
- [5] J. C. Peters, J. P. F. Cherry, J. C. Thomas, L. Baraldo, D. J. Mindiola, W. M. Davis, C. C. Cummins, *J. Am. Chem. Soc.* **1999**, *121*, 10053–10067.
- [6] Q. Cui, D. G. Musaev, M. Svensson, S. Sieber, K. Morokuma, *J. Am. Chem. Soc.* **1995**, *117*, 12366–12367.
- [7] K. M. Neyman, V. A. Nasluzov, J. Hahn, C. R. Landis, N. Rösch, *Organometallics* **1997**, *16*, 995–1000.
- [8] G. Christian, J. Driver, R. Stranger, *Faraday Discuss.* **2003**, *124*, 331–341.
- [9] D. V. Khoroshun, D. G. Musaev, K. Morokuma, *Organometallics* **1999**, *18*, 5653–5660.
- [10] G. Christian, R. Stranger, B. F. Yates, D. C. Graham, *Dalton Trans.* **2005**, 962–968.
- [11] G. Christian, R. Stranger, *Dalton Trans.* **2004**, 2492–2495.
- [12] See the Supporting Information for more computational details.
- [13] $\text{L}=\text{NMe}_2$ was also studied (Supporting Information) and shown to have the same feature as $\text{L}=\text{NH}_2$ (the singlet form is calculated to be 5.3 kJ mol^{-1} more stable than the triplet).
- [14] M. R. A. Blomberg, P. E. M. Siegbahn, *J. Am. Chem. Soc.* **1993**, *115*, 6908–6915.
- [15] K. Tatsumi, R. Hoffmann, *J. Am. Chem. Soc.* **1981**, *103*, 3328–3341.
- [16] D. C. Graham, G. J. O. Beran, M. Head-Gordon, G. Christian, R. Stranger, B. F. Yates, *J. Phys. Chem. A* **2005**, *109*, 6762–6772.
- [17] D. J. Mindiola, K. Meyer, J.-P. F. Cherry, T. A. Baker and C. C. Cummins, *Organometallics* **2000**, *19*, 1622–1624.
- [18] MullPop, R. Pis Diez, National University of La Plata, Argentina.

Received: February 6, 2008
Published online: May 30, 2008